



Graphene Oxide Hot Paper

International Edition: DOI: 10.1002/anie.201510081

German Edition: DOI: 10.1002/ange.201510081



# Graphene Oxide Catalyzed C–H Bond Activation: The Importance of Oxygen Functional Groups for Biaryl Construction

Yongjun Gao<sup>+</sup>, Pei Tang<sup>+</sup>, Hu Zhou, Wei Zhang, Hanjun Yang, Ning Yan, Gang Hu, Donghai Mei, Jianguo Wang,\* and Ding Ma\*

**Abstract:** A heterogeneous, inexpensive, and environmentally friendly graphene oxide catalytic system for the C–H bond arylation of benzene enables the formation of biaryl compounds in the presence of aryl iodides. The oxygen functional groups in these graphene oxide sheets and the addition of KOtBu are essential for the observed catalytic activity. Reactions with various model compounds and DFT calculations confirmed that these negatively charged oxygen atoms promote the overall transformation by stabilizing and activating K<sup>+</sup> ions, which in turns facilitates the activation of the C–I bond. However, the graphene  $\pi$  system also greatly facilitates the overall reaction as the aromatic coupling partners are easily adsorbed.

The direct C–H arylation of benzene, a C–H activation strategy, is a promising reaction to construct aryl–aryl bonds.<sup>[1]</sup> Originally, arylation reactions, such as the Suzuki and Kumada couplings, are based on traditional cross-coupling routes catalyzed by metal complexes. Apart from these water- and oxygen-sensitive reaction systems,<sup>[1]</sup> direct arylation reactions catalyzed by Pd,<sup>[2]</sup> Rh,<sup>[3]</sup> Ru,<sup>[4]</sup> and Ir<sup>[5]</sup> complexes have also been developed. Although their catalytic activities are excellent, the development of cost-efficient and environmentally friendly catalysts to reduce the high production costs as well as the possible heavy-metal contamination remains

essential.<sup>[6]</sup> Green catalytic systems for the formation of aryl–aryl bonds were developed in recent years by switching from precious-metal catalysts to transition-metal catalysts<sup>[7]</sup> or by designing transition-metal-free, organocatalytic systems. Very recently, a variety of metal-free nitrogen- and oxygen-containing compounds, such as *N,N*-dimethylethane-1,2-diamine,<sup>[8]</sup> 1,10-phenanthroline,<sup>[9]</sup> and 4,7-diphenyl-1,10-phenanthroline,<sup>[10]</sup> were shown to effectively promote the C–H arylation of benzene in the presence of a strong base.<sup>[5]</sup> However, the separation and recycling of catalysts in these homogeneous catalytic systems remains a challenge. Furthermore, the catalyst loading is generally as high as 20 %. In some cases, the weight of the catalyst is even greater than that of the substrate.<sup>[9]</sup> The development of heterogeneous, cost-efficient, and environmentally benign catalysts is thus highly desired. Significantly, nanocarbon materials have performed remarkably well as non-metal catalysts in various reactions (“carbocatalysis”).<sup>[11]</sup> Aside from nitrogen-substituted carbon sites,<sup>[12]</sup> specific types of oxygen groups in these carbon materials are the active sites for some of these carbocatalytic reactions.<sup>[13]</sup> Herein, we show that graphene oxide can be employed as an efficient heterogeneous catalyst for the direct C–H arylation of benzene. Both the giant  $\pi$ -conjugated system and oxygen groups with a substantial negative charge are shown to be able to catalyze/promote the reaction. Furthermore, we propose that in this reaction, the type of oxygen species is not the only factor that influences the catalytic activity, as importantly, the type of carbon skeleton that they are connected to has a major impact as well.

As the surface chemistry of graphene is easily manipulated by various chemical modification methods, we tried to use oxygen-rich graphene oxide (GO) as the first metal-free heterogeneous arylation catalyst. The transmission electron microscopy (TEM) image in Figure 1a indicates that GO has a layered structure, and detailed analysis of AFM images (Supporting Information, Figure S1) revealed that our GO sample consists of two to three layers of graphene sheets. Initially, we chose benzene and 4-iodoanisole as the model substrates (Table 1). Almost no product was formed when the reaction was conducted at 100 °C in the absence of catalyst (entry 8). However, coupling product **3a** was formed in 63.8 % yield when a small amount (10 mg) of GO was added to the reaction (entry 1), indicating that GO is indeed a promising catalyst for the arylation of benzene. Full conversion of 4-iodoanisole, and the formation of **3a** in 87.6 % yield, was achieved when the reaction temperature was increased to 120 °C (entry 2). Interestingly, other carbon materials, such as active carbon, carbon black, and natural graphite, were much less active (entries 4–8). As in the

[\*] Dr. Y. Gao,<sup>[+]</sup> P. Tang,<sup>[+]</sup> Dr. W. Zhang, H. Yang, Prof. Dr. D. Ma  
Beijing National Laboratory for Molecular Sciences  
College of Chemistry and Molecular Engineering  
Peking University  
Beijing 100871 (China)  
E-mail: dma@pku.edu.cn

H. Zhou, Prof. Dr. J. Wang  
College of Chemical Engineering  
Zhejiang University of Technology  
Hangzhou 310032 (China)  
E-mail: jgw@zjut.edu.cn

Prof. Dr. N. Yan  
Department of Chemical and Biomolecular Engineering  
National University of Singapore  
4 Engineering Drive 4, 117585 Singapore (Singapore)

Dr. G. Hu  
Israel Chemicals Limited  
Shanghai 200021 (China)

Prof. Dr. D. Mei  
Institute for Integrated Catalysis  
Pacific Northwest National Laboratory  
Richland, WA 99352 (USA)

[+] These authors contributed equally to this work.

Supporting information for this article is available on the WWW under <http://dx.doi.org/10.1002/anie.201510081>.

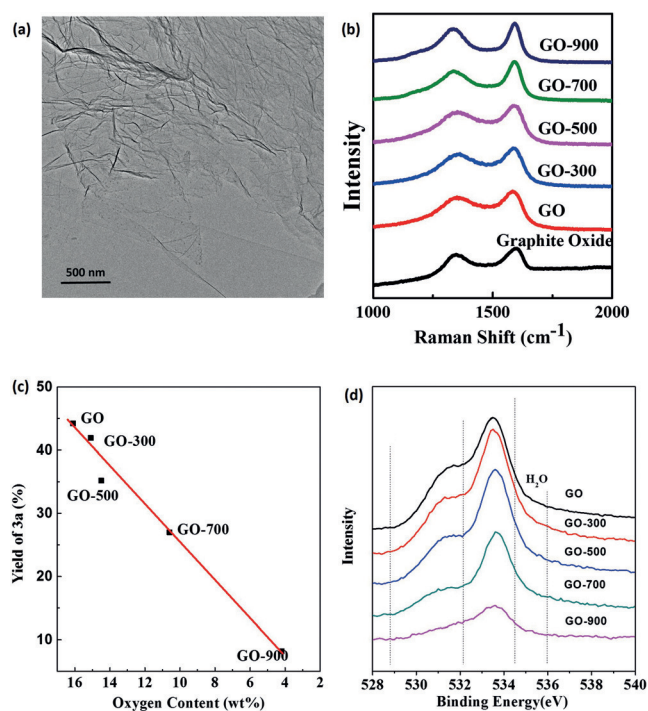


**Figure 1.** a) TEM image of GO. b) Raman spectra of GO and GO-X. c) The dependence of the catalytic activity on the oxygen content, which was determined by XPS. d) XPS O 1s spectra of GO and GO-X.

**Table 1:** Direct GO-catalyzed C–H arylation of benzene.<sup>[a]</sup>

Entry	Catalyst	T [°C]	t [h]	Yield [%]
1	GO	100	24	63.8
2	GO	120	24	87.6
3	GO	120	2	44.2
4	carbon nanotubes	120	24	18.8
5	active carbon	120	24	11.3
6	carbon black	120	24	19.1
7	natural graphite	120	24	8.4
8	–	100	24	trace

[a] Reaction conditions: **1a** (0.4 mmol, 0.096 g), **2** (4 mL), catalyst (0.01 g), KOtBu (1.2 mmol). Yields determined by GC analysis.

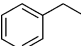
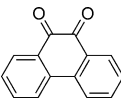
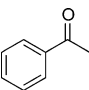
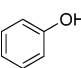
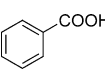
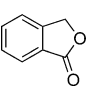
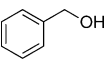
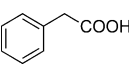
organocatalytic systems,<sup>[8]</sup> potassium cations are essential to this reaction as other bases, such as NaOtBu, are ineffective in promoting the C–H arylation of benzene (Table S1, entry 11). When 18-crown-6 was added to the reaction mixture to trap the K<sup>+</sup> ions, the C–H arylation of benzene with 4-iodoanisole was effectively blocked (Table S2, entry 2). Therefore, we speculated that the K<sup>+</sup> ions, the oxygen species on GO, and possibly the  $\pi$ -conjugated GO system act synergistically to promote the C–H arylation reaction. Moreover, the influence of Mn and Fe impurities in GO is carefully discussed in the Supporting Information (Table S1), and it is GO itself rather than the metal impurities that catalyzes this process.

It has been reported that the oxygen groups on carbon nanotubes and carbon nanodiamonds may account for their catalytic activity in various reactions.<sup>[13,14]</sup> We thus surmised

that the oxygen-containing functional groups on GO may play a key role in the current reaction, although it may differ from that in previously reported reactions. To investigate whether it is one specific kind of oxygen species that is of importance in this process, four catalysts with different oxygen contents were synthesized by controlling the annealing temperatures (300, 500, 700, or 900 °C) of GO (GO-300, GO-500, GO-700, and GO-900, respectively). X-ray photoelectron spectroscopy (XPS) spectra clearly show that the peak intensity of the oxygen species decreases with an increase in treatment temperature (GO: 16.1 wt %; GO-900: 4.2 wt %; for details, see Figure S3 and Table S3). This result is in good agreement with previous reports that stated that high annealing temperatures tend to remove oxygen species from carbon materials.<sup>[15]</sup> Both SEM images (Figure S2) and Raman spectra (Figure 1b) show that aside from the removal of oxygen species, the annealing treatment does not change the structure of GO significantly. Furthermore, the BET surface areas of these GO and GO-X samples are almost the same (Table S2). Subsequent experiments revealed that the lower the oxygen content in GO, the lower its catalytic activity. As all of these GO and GO-X materials possess similar structures, the difference in the oxygen content may be the most important reason to explain their different catalytic activities. Moreover, the yield of desired product (**3a**) depends on the overall oxygen content in the catalyst (Figure 1c), suggesting that the oxygen species play a pivotal role in the direct C–H arylation reaction.

In principle, graphene oxide consists of at least four different oxygen-containing groups on graphene sheets, namely hydroxyl (–OH), epoxide (C–O–C), carbonyl (C=O), and carboxylic acid (–C(O)OH) moieties. Hydroxyl and epoxide moieties, which are distributed over the basal plane of the graphene sheets, are the major oxygen species and preferably react with electrophiles; carbonyl and carboxylic acid groups, which are located at the edges of the graphene sheets, react with nucleophiles.<sup>[16]</sup> The samples prepared at different annealing temperatures were analyzed by XPS (Figure 1d). In all of these samples, the nucleophilic oxygen species are the main functional groups. However, the amount of both electrophilic and nucleophilic oxygen species decreased with an increase in annealing temperature, which actually provides no information that can be used to discriminate the functions of these two types of oxygen species in the reaction. To identify the nature of the crucial oxygen species, a series of oxygen-containing model compounds were tested in the reaction. Compounds where the oxygen atoms are attached either directly to the aryl ring or to a benzylic carbon atom show different catalytic activities (Table 2). Unexpectedly, all of the model compounds with oxygen functional groups directly attached to the benzene ring gave the desired product in very low yield or not at all. On the other hand, when the oxygen functional groups were attached to a benzylic carbon atom, the model compounds catalyzed the desired reaction, and benzyl alcohol was the most active (entries 6–8). As potassium plays a critical role in this C–H bond activation, and the organic catalysts have been speculated to stabilize the reactive K<sup>+</sup> species,<sup>[10]</sup> the fact that oxygen functional groups connected to benzene or benzylic sites show completely

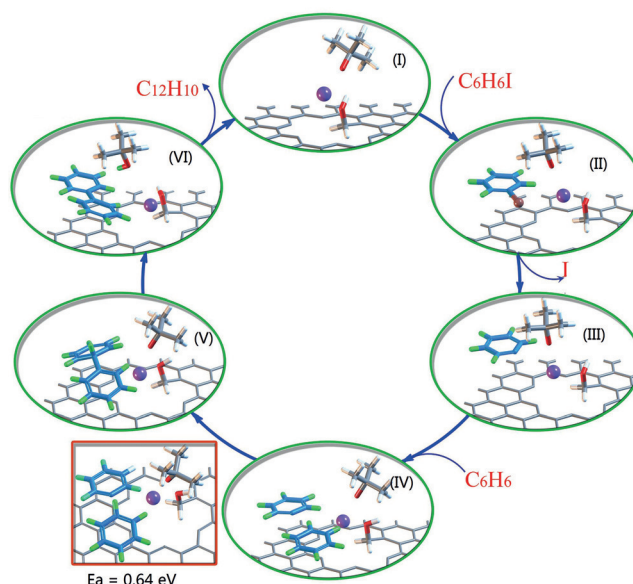
**Table 2:** Catalytic activity and charge analysis of various model compounds.<sup>[a]</sup>

Entry	Catalyst	Charge (e)	Yield [%]
1		CH <sub>2</sub> (−0.03)	–
2		O (−2.10)	–
3		O (−2.22)	3.2
4		O (−1.13)	–
5		O (C=O) (−0.85) O (C–O) (−0.85)	–
6		O (C=O) (−2.10) O (C–O) (−0.64) H (CH <sub>2</sub> ) (0.21)	9.7
7		O (−0.88) H (CH <sub>2</sub> ) (0.32)	22.3
8		O (C=O) (−2.0) O (C–O) (−0.85) H (CH <sub>2</sub> ) (0.06)	9.4

[a] Reaction conditions: **1a** (0.4 mmol), **2** (4 mL), catalyst (0.3 mmol), KO<sup>t</sup>Bu (1.2 mmol), 120 °C, 2 h. Yields determined by GC analysis.

different catalytic activities inspired us to investigate whether the  $\pi$  system of the catalyst influences the reactivity of the oxygen functional groups. A Bader charge analysis (Table 2) confirmed that the negative charge is always concentrated on the oxygen atoms. For example, the oxygen atom in benzyl alcohol (entry 7) has a negative charge of  $-0.88e$ , whereas those in acetophenone, phenol, and benzoic acid (entries 3–5) have charges of  $-2.22e$ ,  $-1.13e$ , and  $-0.85e$ , respectively. The negative charge can stabilize  $K^+$  ions. Significantly, for compounds with benzylic  $CH_2$  groups, these hydrogen atoms were positively charged while the oxygen atoms were negatively charged (entries 6–8).  $K^+$  ions could be accommodated on and activated by the negative charge of the oxygen groups. While activated  $K^+$  ions can attack the C–I bond in iodobenzene, the positively charged benzylic hydrogen atoms facilitate the stabilization of  $C_6H_5$  radicals, aside from the  $\pi$ – $\pi$  interaction stabilization. Therefore, in this process, model compounds with oxygen functional groups at benzylic sites not only stabilize  $K^+$  ions by means of their negatively charged oxygen atoms but also facilitate the stabilization of  $C_6H_5$  radicals (Figure S4); therefore, they display good catalytic activity in these arylation reactions.

We then analyzed the exact role of GO, and of the GO oxygen functional groups and  $K^+$  ions, in particular, in the arylation of benzene by DFT calculations. As benzyl alcohol

**Figure 2.** Mechanism proposed for the GO-catalyzed arylation reaction.

was a particularly active model system, we decided to focus on a GO nanopore (the edge of graphene; Figure 2). Without hydroxy groups, the interaction between KO<sup>t</sup>Bu and graphene is very weak. Instead, as shown in Figure 2,  $K^+$  can strongly interact with oxygen species at the edge of a graphene nanopore (**I**; the adsorption energy,  $E_{ad}$ , is  $-0.96$  eV). The distance between a  $K^+$  ion and the oxygen atom of an ether O<sup>t</sup>Bu moiety is 2.53 Å, whereas the distance between  $K^+$  and a hydroxy oxygen atom is 2.57 Å. At the same time, the  $\pi$ – $\pi$  interactions between the  $\pi$  system of graphene and that of iodobenzene enable the adsorption of the latter on the same graphene surface (**II**,  $E_{ad} = -0.97$  eV).<sup>[17]</sup> The charge of the immobilized  $K^+$  ion is 0.89 e owing to the electron transfer between K and the oxygen group, which is beneficial to the subsequent activation of iodobenzene. Indeed, the iodine–carbon bond of iodobenzene can be easily activated by attack of a  $K^+$  ion, which leads to the formation of a  $C_6H_5$  radical. The benzene radical is stabilized by the  $\pi$  system of graphene as well as the positively charged hydrogen atoms (**III**;  $E_{ad} = -1.29$  eV). This intermediate then reacts with adsorbed benzene (**IV**;  $E_{ad} = -0.76$  eV) with a moderate activation energy (0.64 eV). After proton transfer, biphenyl is formed (**VI**). Significantly, aside from the immobilization of  $K^+$  ions by the oxygen groups at the edge of GO, GO also attracts the aromatic molecules through  $\pi$ – $\pi$  interactions and thus provides a platform for the reactants. The radical nature of the reaction mechanism was further confirmed by radical trapping experiments (Table S4).

Finally, we investigated whether GO can be used as a catalyst for other benzene arylation reactions by examining a range of aryl iodides (ArI; Table 3). In general, electron-rich aryl iodides were more reactive than electron-neutral ones. Aryl iodides with an *ortho* substituent were less reactive than those with *para* substituents owing to steric hindrance. For example, 4-iodoanisole (**1a**) provided **3a** in 87.6% yield, whereas **3e** was only formed in 61.9% yield from 2-



**Table 3:** GO-catalyzed direct C–H arylation of benzene with ArX.<sup>[a]</sup>

$\text{ArX} + \text{C}_6\text{H}_6 \xrightarrow[120^\circ\text{C}]{\text{GO, KOtBu}} \text{Ar-C}_6\text{H}_5$					
	1	2		3	
Entry	Ar	X	1	Product	Yield [%]
1	4-MeOC <sub>6</sub> H <sub>4</sub>	I	1a	3a	87.6
2	C <sub>6</sub> H <sub>5</sub>	I	1b	3b	81.6
3	4-EtC <sub>6</sub> H <sub>4</sub>	I	1c	3c	80.7
4	4- <i>i</i> PrC <sub>6</sub> H <sub>4</sub>	I	1d	3d	71.7
5	2-MeOC <sub>6</sub> H <sub>4</sub>	I	1e	3e	61.9
6	3-MeOC <sub>6</sub> H <sub>4</sub>	I	1f	3f	29.4
7	4-MeC <sub>6</sub> H <sub>4</sub>	I	1g	3g	84.4
8	2-MeC <sub>6</sub> H <sub>4</sub>	I	1h	3h	57.5
9	3-MeC <sub>6</sub> H <sub>4</sub>	I	1i	3i	80.1
10	1-naphthyl	I	1j	3j	52.3
11	4-PhC <sub>6</sub> H <sub>4</sub>	I	1k	3k	92.4
12	4-ClC <sub>6</sub> H <sub>4</sub>	I	1l	3k	69.2
13	4-MeOC <sub>6</sub> H <sub>4</sub>	Br	1m	3a	7.9
14	C <sub>6</sub> H <sub>5</sub>	Br	1n	3b	3.2
15	C <sub>6</sub> H <sub>5</sub>	Cl	1o	3b	0

[a] Reaction conditions: **1** (0.4 mmol), **2** (4 mL), catalyst (0.01 g), KOtBu (1.2 mmol), 120 °C, 24 h. Yields determined by GC analysis.

iodoanisole (**1e**; entries 1 and 5). Unexpectedly, **3f** was only furnished in 29.4 % yield from 3-iodoanisole (**1f**; entry 6). This result is not in accordance with literature reports.<sup>[8]</sup> We speculate that a combination of electronic and steric effects decrease the reactivity of **1f** when the methoxy group is located at the *meta* position. The coupling of benzene with 1-iodonaphthalene was also less efficient. Surprisingly, 4-chlorobiphenyl was only formed in 4.5 % yield in the reaction of 4-chloro-1-iodobenzene (**1l**) with benzene. Instead, a large amount of *para*-terphenyl **3k** was detected in the reaction mixture, indicating that dehalogenation had occurred (entry 12). Aryl bromides and chlorides were also tested, but gave the desired products in reduced yields (entry 13–15). The recyclability of these GO catalysts was also tested. After five cycles, the catalyst had maintained more than 60 % of its original activity, and the catalyst could be easily regenerated by reoxidation (Figure S6).

In summary, a new nanocarbon-based catalytic system for the direct C–H arylation of benzene has been developed. To the best of our knowledge, this is the first report of carbocatalysis for direct C–H arylation with formation of the coupling products in high yields. However, this work has also provided insights into the roles of the various functional groups on nanocarbon materials.

## Experimental Section

**Materials:** Graphitic oxide was generated from natural flake graphite according to a modified Hummers method.<sup>[18]</sup> Graphitic oxide was heated in a quartz tube (H<sub>2</sub> flow, 30 mL min<sup>−1</sup>) to 250 °C (20 °C min<sup>−1</sup>) to obtain graphene oxide.

**Catalytic reaction:** ArI (0.4 mmol), catalyst (0.01 g), KOtBu (1.2 mmol), and benzene (4 mL) were added to a 35 mL glass reactor sealed with a Teflon lid. The reaction mixture was heated to 120 °C for 24 h unless otherwise specified. After cooling to room temperature, *n*-dodecane (0.05 g) was added as an internal standard, and then CH<sub>2</sub>Cl<sub>2</sub>

(10 mL) was added. The products were analyzed by an Agilent 7820 GC with a HP-INNOWax capillary column and an Agilent GC-MS.

DFT calculations were performed on the basis of spin polarized DFT within the generalized gradient approximation (GGA-PBE) including van der Waals (vdw) interactions, as implemented in the Vienna Ab Initio Simulation Package (VASP).

## Acknowledgements

This work received financial support from the Natural Science Foundation of China (21173009, 21222306, 91334103, and 21136001) and the 973 Project (2011CB201402, 2013CB933100, and 2013CB733501). Soft X-ray adsorption measurements were done at the NSRF.

**Keywords:** arylation · carbon · graphene oxide · heterogeneous catalysis

**How to cite:** *Angew. Chem. Int. Ed.* **2016**, 55, 3124–3128

*Angew. Chem.* **2016**, 128, 3176–3180

- [1] a) D. Alberico, M. E. Scott, M. Lautens, *Chem. Rev.* **2007**, 107, 174–238; b) T. L. Chan, Y. N. Wu, P. Y. Choy, F. Y. Kwong, *Chem. Eur. J.* **2013**, 19, 15802–15814.
- [2] a) M. Lafrance, K. Fagnou, *J. Am. Chem. Soc.* **2006**, 128, 16496–16497; b) T. W. Lyons, M. S. Sanford, *Chem. Rev.* **2010**, 110, 1147–1169.
- [3] S. Proch, R. Kempe, *Angew. Chem. Int. Ed.* **2007**, 46, 3135–3138; *Angew. Chem.* **2007**, 119, 3196–3199.
- [4] L. Ackermann, J. Pospech, H. K. Potukuchi, *Org. Lett.* **2012**, 14, 2146–2149.
- [5] K.-i. Fujita, M. Nonogawa, R. Yamaguchi, *Chem. Commun.* **2004**, 1926–1927.
- [6] A. Lei, W. Liu, C. Liu, M. Chen, *Dalton Trans.* **2010**, 39, 10352–10361.
- [7] a) W. Liu, H. Cao, A. Lei, *Angew. Chem. Int. Ed.* **2010**, 49, 2004–2008; *Angew. Chem.* **2010**, 122, 2048–2052; b) F. Vallée, J. J. Mousseau, A. B. Charette, *J. Am. Chem. Soc.* **2010**, 132, 1514–1516.
- [8] W. Liu, H. Cao, H. Zhang, H. Zhang, K. H. Chung, C. He, H. Wang, F. Y. Kwong, A. Lei, *J. Am. Chem. Soc.* **2010**, 132, 16737–16740.
- [9] E. Shirakawa, K.-i. Itoh, T. Higashino, T. Hayashi, *J. Am. Chem. Soc.* **2010**, 132, 15537–15539.
- [10] C. L. Sun, H. Li, D. G. Yu, M. A. Yu, X. A. Zhou, X. Y. Lu, K. Huang, S. F. Zheng, B. J. Li, Z. J. Shi, *Nat. Chem.* **2010**, 2, 1044–1049.
- [11] a) S. Navalón, A. Dhakshinamoorthy, M. Alvaro, H. Garcia, *Chem. Rev.* **2014**, 114, 6179–6212; b) D. S. Su, S. Perathoner, G. Centi, *Chem. Rev.* **2013**, 113, 5782–5816; c) C. L. Su, K. P. Loh, *Acc. Chem. Res.* **2013**, 46, 2275–2285; d) H. P. Jia, D. R. Dreyer, C. W. Bielawski, *Tetrahedron* **2011**, 67, 4431–4434; e) D. R. Dreyer, C. W. Bielawski, *Chem. Sci.* **2011**, 2, 1233–1240; f) D. R. Dreyer, A. D. Todd, C. W. Bielawski, *Chem. Soc. Rev.* **2014**, 43, 5288–5301; g) D. W. Boukhvalov, D. R. Dreyer, C. W. Bielawski, Y. W. Son, *ChemCatChem* **2012**, 4, 1844–1849; h) J. H. Yang, G. Sun, Y. J. Gao, H. B. Zhao, P. Tang, J. Tan, A. H. Lu, D. Ma, *Energy Environ. Sci.* **2013**, 6, 793–798.
- [12] a) Y. J. Gao, G. Hu, J. Zhong, Z. J. Shi, Y. S. Zhu, D. S. Su, J. G. Wang, X. H. Bao, D. Ma, *Angew. Chem. Int. Ed.* **2013**, 52, 2109–2113; *Angew. Chem.* **2013**, 125, 2163–2167; b) W. J. Li, Y. J. Gao, W. L. Chen, P. Tang, W. Z. Li, Z. J. Shi, D. S. Su, J. G. Wang, D. Ma, *ACS Catal.* **2014**, 4, 1261–1266.

- [13] a) J. Zhang, X. Liu, R. Blume, A. H. Zhang, R. Schlögl, D. S. Su, *Science* **2008**, 322, 73–77; b) G. Mestl, N. I. Maksimova, N. Keller, V. V. Roddatis, R. Schlögl, *Angew. Chem. Int. Ed.* **2001**, 40, 2066–2068; *Angew. Chem.* **2001**, 113, 2122–2125.
- [14] J. Zhang, D. S. Su, R. Blume, R. Schlögl, R. Wang, X. G. Yang, A. Gajovic, *Angew. Chem. Int. Ed.* **2010**, 49, 8640–8644; *Angew. Chem.* **2010**, 122, 8822–8826.
- [15] P. Tang, G. Hu, Y. J. Gao, W. J. Li, S. Y. Yao, Z. Y. Liu, D. Ma, *Sci. Rep.* **2014**, 4, 5901.
- [16] B. Frank, R. Blume, A. Rinaldi, A. Trunschke, R. Schlögl, *Angew. Chem. Int. Ed.* **2011**, 50, 10226–10230; *Angew. Chem.* **2011**, 123, 10408–10413.
- [17] J. H. Yang, Y. J. Gao, W. Zhang, P. Tang, J. Tan, A. H. Lu, D. Ma, *J. Phys. Chem. C* **2013**, 117, 3785–3788.
- [18] W. S. Hummers, R. E. Offeman, *J. Am. Chem. Soc.* **1958**, 80, 1339–1339.

Received: October 29, 2015

Published online: January 6, 2016